QM/MM Studies on Photoisomerization Dynamics of Azobenzene Chromophore Tethered to a DNA Duplex: Local Unpaired Nucleobase Plays a Crucial Role

Dan Wu,[a] Ya-Ting Wang,[a] Wei-Hai Fang,[a] Ganglong Cui,*[a] and Walter Thiel[b]

Abstract: The photoresponsive azobenzene-tethered DNAs have received growing experimental attention because of their potential applications in biotechnology and nanotechnology; however, little is known about the initial photoisomerization of azobenzene in these systems. Herein we have employed quantum mechanics/molecular mechanics (QM/MM) methods to explore the photoisomerization dynamics of an azobenzene-tethered DNA duplex. We find that in the S_1 state the *trans–cis* photoisomerization path is much steeper in DNA than in vacuo, which makes the photoisomerization much faster in the DNA environment. This acceleration is primarily caused by complex steric interactions between azobenzene and the nearby unpaired thymine nucleobase, which also change the photoisomerization mechanism of azobenzene in the DNA duplex.

Keywords: azobenzene · DNA · mechanics · photoswitches · surface-hopping dynamics

Molecular photoswitches have been extensively used in a variety of applications ranging from materials science to biology.[1] Among the most studied photoswitchable compounds are azobenzenes, which are easily synthesized and highly stable.[2] They have high extinction coefficients and isomerization quantum yields, thereby allowing repeated photoswitching with low-intensity light. Photoinduced isomerization changes the shape of these azobenzenes significantly, in particular the end-to-end distance, which has been exploited in tuning the folding and unfolding of peptides and proteins.[3]

Photoresponsive azobenzene-tethered DNA/RNAs have in recent years attracted growing attention for their potential applications in biotechnology and nanotechnology,[4] for example in photoregulating the DNA duplex/triplex formation and dissociation,[5] the transcription by T7-RNA polymerase,[6] the RNA digestion by RNase H,[7] the DNA polymerase reaction by oligonucleotides,[8] the enzymatic activity by telomere DNA,[9] the RNA cleavage by deoxyribozyme,[10] and the ion transport of biomimetic DNA-based channels.[11]

Previous experimental studies are almost entirely focused on exploring structure-function and thermodynamics properties, such as melting temperatures, integrated photokinetic factors, etc.[12] Very little is known about the initial photoisomerization dynamics of azobenzene in these constrained DNA/RNAs, which is at the heart of understanding the underlying photoregulation mechanism and a prerequisite for the rational design of more excellent azobenzene-tethered DNA/RNAs. Such microscopic information can be provided by reliable theoretical methods. However, except for classical force-field simulations,[13] the photoisomerization dynamics in the azobenzene-DNA systems has not yet been explored computationally. In this communication we report a quantum mechanics/molecular mechanics (QM/MM) study of the photoisomerization mechanism and dynamics of an azobenzene chromophore tethered to a DNA duplex in aqueous solution (see Supporting Information for simulation details and Figure 1 for QM/MM partitioning); the choice of this system was motivated by a recent experimental study showing remarkable photoswitching properties.[12c] After submission of our manuscript, a related semiempirical QM/MM study became available on a preprint

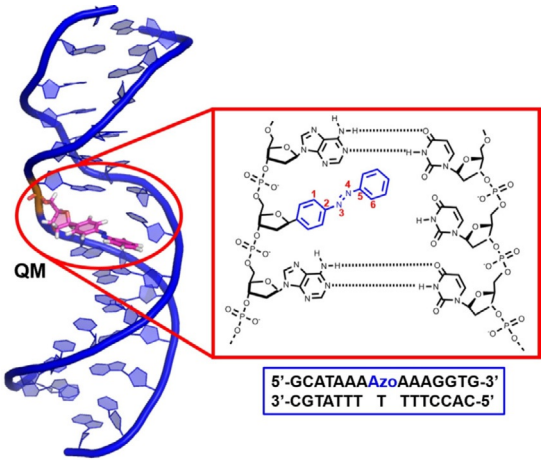

Figure 1. Azobenzene-tethered DNA duplex studied in recent experiments.[12c] Also shown are the DNA nucleic acid sequences (blue box) and the related QM/MM partitioning (red box: QM in blue and MM in black).

[a] *D. Wu, Y.-T. Wang, Prof. Dr. W.-H. Fang, Prof. Dr. G. Cui*
Key Laboratory of Theoretical and Computational Photochemistry, Ministry of Education
College of Chemistry
Beijing Normal University
Beijing 100875 (China)
E-mail: ganglong.cui@bnu.edu.cn

[b] *Prof. Dr. W. Thiel*
Max-Planck-Institut für Kohlenforschung
Kaiser-Wilhelm-Platz 1, 45470 Mülheim an der Ruhr (Germany)

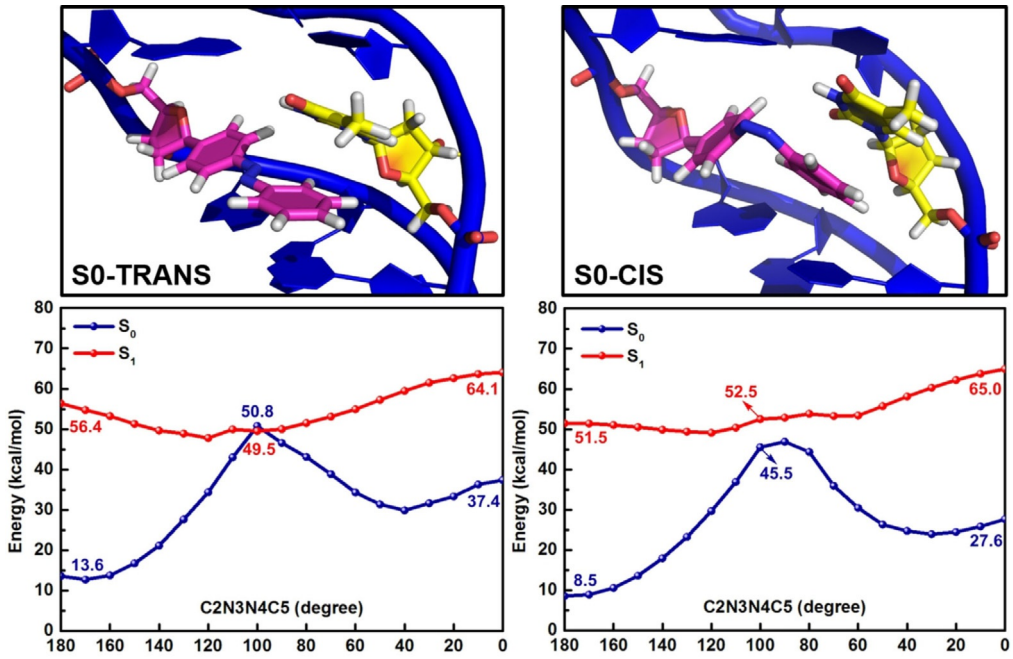

Figure 2. (Top) QM(CASSCF)/MM optimized minimum-energy structures of a DNA duplex with the azobenzene chromophore in the (left) *trans* and (right) *cis* conformation in the S_0 state. (Bottom) QM(CASPT2)/MM computed photoisomerization pathways in (left) a **DNA duplex** and (right) in the **gas phase** in the S_1 (relaxed) and S_0 (unrelaxed) states. See the Supporting Information for analogous plots for the same DNA duplex without the nearby thymine nucleobase.

server, which addressed the photoisomerization dynamics of two representative RNA-azobenzene complexes using surface hopping.[14]

At the QM(CASSCF)/MM level, we have optimized the stable *trans* and *cis* azobenzene structures in the DNA environment, which are labeled as S0-TRANS and S0-CIS in Figure 2. The central N=N double bond length of S0-TRANS [S0-CIS] is computed to be 1.27 [1.23] Å, which is similar to 1.24 [1.24] Å in the gas phase; in addition, the C2N3N4C5 dihedral angles are also close to those in the gas phase, 173.7° [1.7°] versus 180° [4.2°].[15a] In stark contrast, the nearby dihedral angles relevant to the photoisomerization markedly differ from those in the gas phase due to steric interactions between the azobenzene and the nearby nucleobases. For example, the C1C2N3N4 and N3N4C5C6 dihedral angles of S0-TRANS [S0-CIS] in the DNA environment are computed to be 164.0° [−91.0°] and 173.8° [−168.9°], respectively, which deviate from 180.0° [-125.2°] and 180.0° [−125.2°] in the gas phase.[15a] These significant structural differences do not alter the relative stabilities of S0-TRANS and S0-CIS. At the QM(MS-CASPT2)/MM level, S0-TRANS is predicted to be 12.9 kcal mol^{-1} lower in energy than S0-CIS, which is close to the value of 11.9 kcal mol^{-1} calculated by the CASPT2 method in the gas phase.[15a]

In addition, we have computed the vertical excitation energies at the Franck-Condon points for S0-TRANS and S0-CIS. The lowest excited singlet state stems from an n→π* electronic excitation in both cases (see Figure S2 for the relevant orbitals). The vertical excitation energy to this ^{1}nπ* state in S0-TRANS [S0-CIS] is computed to be 62.4 [60.4] kcal mol^{-1} at the QM(CASPT2)/MM level, close to the value of 57.7 [62.5] kcal mol^{-1} calculated in the gas phase[15a] and the experimentally measured absorption band maximum of 445 nm (64.3 kcal mol^{-1}).[13d] MO analysis shows that this excited singlet state is primarily composed of the HOMO–LUMO electronic configuration (Figure S2). The HOMO is a lone-pair n orbital at the two nitrogen atoms and the LUMO is the antibonding $\pi^*_{N=N}$ orbital of the azo group.

To explore the photoisomerization of azobenzene in the DNA surroundings, we have computed the photoisomerization reaction path in the S_1 state for the internal rotation described by the central C2N3N4C5 dihedral angle. As seen in the bottom-left panel of Figure 2, there exists an S_1/S_0 conical intersection region in the vicinity of 90°, where both electronic states are energetically quasi-degenerate at the QM(CASPT2)/MM level. The corresponding S_1/S_0 minimum-energy conical intersection structure has been fully optimized at the QM(OM2/MRCI)/MM level (Table S3 and Figure S3). In this optimized structure (labeled S1S0-CI), the central C2N3N4C5 dihedral angle is 101.5°, slightly larger than the gas-phase value of 94.0°.[15] The C1C2N3N4 and N3N4C5C6 dihedral angles are −170.1° and 166.4°, respectively. At the QM(CASPT2)/MM level, the S_1 and S_0 energies at S1S0-CI are 50.8 and 49.5 kcal mol^{-1}, which shows that these two electronic states are still quasi-degenerate at the higher computational level; the S_1 energy of S1S0-CI is ca. 12 kcal mol^{-1} lower than that at the *trans* Franck-Condon point (see Table S4) so that this conical intersection is energetically accessible. Therefore, it is expected to play a crucial role in the decay of the S_1 state to the S_0 state during the photodynamics of azobenzene in the DNA surroundings.

From the bottom-left panel of Figure 2, one can see that both *trans–cis* and *cis–trans* photoisomerization paths are barrierless in the S_1 state. For the sake of comparison, we have

also computed the relevant S_1 photoisomerization path in the gas phase at the CASPT2 level (see the bottom-right panel of Figure 2). It is obvious that the *cis–trans* photoisomerization paths in the gas phase and DNA have similar steepness (energies decreasing from 65.0 to 52.5 kcal mol^{-1} and from 64.1 to 50.8 kcal mol^{-1}, respectively). By contrast, the S_1 *trans–cis* photoisomerization path is much steeper in the DNA surroundings than in the gas phase, where it is nearly flat with respect to the variation of the central C2N3N4C5 dihedral angle. Moreover, one can see that the S_0 and S_1 states do not become degenerate along the S_1 minimum-energy reaction path in vacuum. At a dihedral angle of about 100°, the $S_1 \rightarrow S_0$ energy gap is computed to be 7.0 kcal mol^{-1} in the gas phase. This situation changes in the DNA environment where a quasi-degenerate S_1/S_0 conical intersection is observed (energy gap of 1.3 kcal mol^{-1}, see above). Taken together, one can expect that the *trans–cis* photoisomerization will be much faster in the DNA than in the gas phase (see below).

To further confirm this viewpoint and to explore the excited-state properties of the *trans–cis* azobenzene photoisomerization in the DNA, we have carried out QM(OM2/MRCI)/MM nonadiabatic dynamics runs starting from the *trans* region (200 trajectories). Counting the number of trajectories arriving at the *cis* and *trans* conformers, we estimate the quantum yield of the *trans–cis* photoisomerization to be 0.42, which is higher than those predicted in the gas and solution phases (0.17 and 0.20–0.25, respectively).[15g]

We have analyzed the distribution of the C1C2N3N4, C2N3N4C5, and N3N4C5C6 dihedral angles at the starting points (blue squares) and the $S_1 \rightarrow S_0$ hopping points (red circles), as shown in Figure 3. At the beginning, the distribution of the central C2N3N4C5 dihedral angle ranges from 140° to 200° with the center at about 170°. This is consistent with the structure of S0-TRANS, where the C2N3N4C5 dihedral angle is computed to be 173.7° and 176.7° at QM(CASSCF)/ MM and QM(OM2/MRCI)/MM levels, respectively. The starting distribution of the C1C2N3N4 dihedral angle, between 210° and 110° (center at ca. 160°), is slightly wider than that of N3N4C5C6 dihedral angle, between 200° and 130° (center at ca. 165°). This indicates that the rotational motion of the right phenyl group of azobenzene (Figure 2) is more hindered by the nearby thymine nucleobase than that of the left phenyl group. When going from the starting to hopping points, the centroid of the distribution of the N3N4C5C6 dihedral angle changes only slightly, from 170° to 165° (see the top-right panel of Figure 3), whereas that of the C1C2N3N4 dihedral angle changes visibly, from 160° to 200° (see the top-left panel of Figure 3). This further confirms that the rotational motion along the C1C2N3N4 dihedral angle is less constrained than that of the N3N4C5C6 dihedral angle. It should be stressed that in previous dynamics simulations in the gas and solution phases, the rotational motions along the C1C2N3N4 and N3N4C5C6 dihedral angles were found to be unrestrained and of equal importance in the photodynamics of azobenzene.[15g] The present work demonstrates that the DNA environment can inhibit one of the rotational motions (see below).

Figure S8 shows the time-dependent population of the S_1 and S_0 states. In the first 50 fs after photoexcitation, the system relaxes in the S_1 state from the Franck-Condon region to the minimum; thereafter, the trajectories start continually hopping to the S_0 state. Until the end of the 500 fs simulations, 90% of the trajectories hop from the initially populated S_1 state to the S_0 state. Provided that the $S_1 \rightarrow S_0$ internal conversion is a first-order process, the S_1 excited-state lifetime is estimated to be 394 fs. We note that such ultrafast *trans–cis* photoisomerizations are not observed in azobenzene cross-linked peptides (lifetimes of ca. 1 ps).[15] Apparently, the *trans–cis* photoisomerization is accelerated by the interactions between the azobenzene and the DNA environment. This is in contrast to the situation in the recently investigated RNA-azobenzene complexes, in which the *trans–cis* photoisomerization was found to be slowed down significantly to a time scale of about 15 ps.[14] This highlights the decisive impact of the different DNA and RNA environments.

What is the driving force for such acceleration? Careful inspection of the structural features near the azobenzene suggests that the steric interaction between the right phenyl group of the azobenzene and the nearby thymine nucleobase could be responsible for this phenomenon (Figure 4). The importance of such steric interactions with an opposite base has already been pointed out in previous force-field work.[13c] To address this issue, we have carried out QM/MM electronic structure calculations and dynamics simulations for an analogous DNA duplex without this nearby nucleobase. It is evident from Figures S5 and S6 that at the QM(CASPT2)/MM level the S_1 photoisomerization path for *cis–trans* photoisomerization

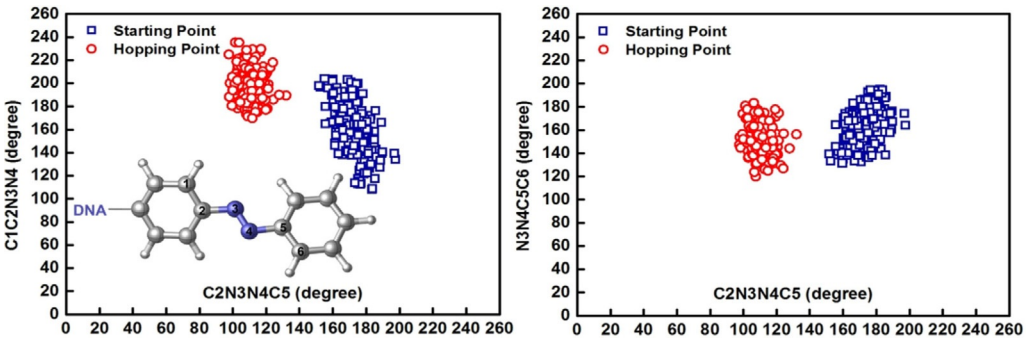

Figure 3. Distribution of (left) the C1C2N3N4 and C2N3N4C5 dihedral angles, and (right) the C2N3N4C5 and N3N4C5C6 dihedral angles at the starting points (blue squares) and the $S_1 \rightarrow S_0$ hopping points (red circles).

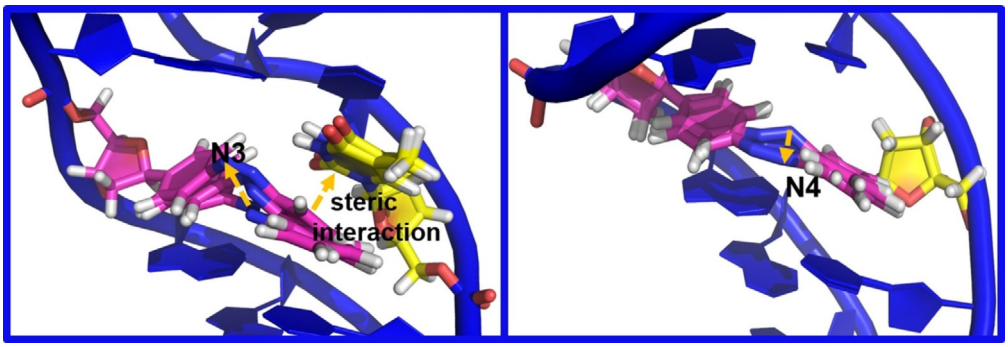

Figure 4. Spatial superpositions of S0-TRANS, S1S0-CIS, and S0-CIS structures in the DNA duplex (left) with an unpaired thymine nucleobase and without it (right). The out-of-plane motions of the N3 and N4 atoms of the azobenzene play different roles for the photoisomerization in the two DNA environments.

looks similar in the unmodified and modified DNA duplexes. However, the *trans–cis* photoisomerization path is different in the unmodified and modified DNAs (Figures S5 and S6). Due to the strong steric interaction between the right phenyl group of the azobenzene and the nearby thymine nucleobase (Figure 4), the S_1 energy profile for the *trans–cis* path is much steeper in the unmodified than in the modified DNA (without the thymine nucleobase). This steric interaction is thus the driving force that re-shapes the S_1 *trans–cis* potential energy surface and accelerates the *trans–cis* photoisomerization. This is again confirmed by QM(OM2/MRCI)/MM dynamics simulations. In 200 trajectories, we do not observe any $S_1 \rightarrow S_0$ excited-state decay nor any *trans–cis* photoisomerization during the 500 fs simulations. This is qualitatively different from the situation in the unmodified DNA environment where ca. 90% of the trajectories decay to the S_0 state (see above). Both the electronic structure calculations and the dynamics simulations thus support the motion that the steric interaction between one phenyl group of the azobenzene and the nearby thymine is responsible for the acceleration of the *trans–cis* photoisomerization.

In addition, this steric interaction also makes the *trans–cis* photoisomerization mechanism of the azobenzene in the unmodified DNA different from that in the modified one. Figure 4 shows spatial superpositions of S0-TRANS, S1S0-CIS, and S0-CIS structures in these two DNA duplexes. It is clear from the left panel that in the unmodified DNA the hula-twist photoisomerization process is dominantly driven by the N3 atom of the azo N=N group because the rotational motion along the C1C2N3N4 dihedral angle is less constrained than that along the N3N4C5C6 dihedral angle (as discussed above). Removal of the nearby thymine nucleobase reduces this steric interaction and enables rotational motion along the N3N4C5C6 dihedral angle. As a result, the N4 atom drives the hula-twist motion in the modified DNA (see the right panel). This demonstrates that the two nitrogen atoms can play different roles in the photoinduced hula-twist of the central N=N double bond and that the local environment can be of decisive importance in regulating the excited-state relaxation paths of azobenzene in the confined DNA surroundings.

To summarize, we have employed combined QM/MM electronic structure calculations and nonadiabatic dynamics simulations to study the photoisomerization mechanism and excited-state decay dynamics of an azobenzene that is covalently tethered to a DNA duplex. We find that the *trans–cis* photoisomerization path in the S_1 state is much steeper in the DNA surroundings than in the gas phase; whereas, the *cis–trans* path is similar in both situations. This enhanced steepness makes the *trans–cis* photoisomerization much faster in the DNA than in vacuum, which is confirmed by our subsequent surface-hopping dynamics simulations. Moreover, we find that the enhanced steepness of the *trans–cis* photoisomerization path in the DNA duplex is mainly caused by the steric interaction between the phenyl group of the azobenzene and the corresponding unpaired thymine nucleobase, which is supported by further electronic structure calculations and nonadiabatic dynamics simulations on an analogous DNA duplex without this unpaired nucleobase. This steric interaction also changes the *trans–cis* photoisomerization mechanism of azobenzene, since the two nitrogen atoms are found to play different roles in driving the hula-twist motion of the central N=N double bond in the unmodified and modified DNA duplexes. Finally, we emphasize that the focus of our present study is on exploring the initial photoisomerization dynamics of two representative DNA-azobenzene complexes[12c] and the effects of the local DNA environment on the S_1 dynamics; further work is required to address computationally the efficiency of these complexes for DNA photocontrol.

In more general terms, the present study shows that complicated biological surroundings can re-shape excited-state potential energy surfaces of chromophores, thereby tuning and even significantly changing their photodynamics. We hope that these mechanistic insights will advance the understanding and design of azobenzene-tethered DNA/RNAs in biotechnology and nanotechnology.[4–12]

Acknowledgements

This work has been supported by the grants NSFC 21522302 (G.C.) and NSFC 21520102005 (G.C. and W.F.), and an ERC Advanced grant (OMSQC, W.T.).

Conflict of interest

The authors declare no conflict of interest.

[1] a) Y. N. Teo, E. T. Kool, *Chem. Rev.* **2012**, *112*, 4221 – 4245; b) W. Szymański, J. M. Beierle, H. A. V. Kistemaker, W. A. Velema, B. L. Feringa, *Chem. Rev.* **2013**, *113*, 6114 – 6178; c) A. S. Lubbe, W. Szymanski, B. L. Feringa, *Chem. Soc. Rev.* **2017**, *46*, 1052 – 1079.

[2] A. Beharry, G. Woolley, *Chem. Soc. Rev.* **2011**, *40*, 4422 – 4437.

[3] a) F. Zhang, A. Zarrine-Afsar, M. Al-Abdul-Wahid, R. Prosser, A. Davidson, G. Woolley, *J. Am. Chem. Soc.* **2009**, *131*, 2283 – 2289; b) F. Zhang, K. Timm, K. Arndt, G. Woolley, *Angew. Chem. Int. Ed.* **2010**, *49*, 3943 – 3946; *Angew. Chem.* **2010**, *122*, 4035 – 4038.

[4] a) Y. M. Kim, J. A. Phillips, H. P. Liu, H. Z. Kang, W. H. Tan, *Proc. Natl. Acad. Sci. USA* **2009**, *106*, 6489 – 6494; b) X. L. Wang, J. Huang, Y. Y. Zhou, S. Y. Yan, X. C. Weng, X. J. Wu, M. G. Deng, X. A. Zhou, *Angew. Chem. Int. Ed.* **2010**, *49*, 5305 – 5309; *Angew. Chem.* **2010**, *122*, 5433 – 5437; c) M. McCullagh, I. Franco, M. A. Ratner, G. C. Schatz, *J. Am. Chem. Soc.* **2011**, *133*, 3452 – 3459; d) M. A. Kienzler, A. Reiner, E. Trautman, S. Yoo, D. Trauner, E. Y. Isacoff, *J. Am. Chem. Soc.* **2013**, *135*, 17683 – 17686; e) Y. Kamiya, H. Asanuma, *Acc. Chem. Res.* **2014**, *47*, 1663 – 1672; f) J. Thevarpadam, I. Bessi, O. Binas, D. P. N. Goncalves, C. Slavov, H. R. A. Jonker, C. Richter, J. Wachtveitl, H. Schwalbe, A. Heckel, *Angew. Chem. Int. Ed.* **2016**, *55*, 2738 – 2742; *Angew. Chem.* **2016**, *128*, 2788 – 2792; g) Y. Nakasone, H. Ooi, Y. Kamiya, H. Asanuma, M. Terazima, *J. Am. Chem. Soc.* **2016**, *138*, 9001 – 9004; h) S. A. Reis, B. Ghosh, J. A. Hendricks, D. M. Szantai-Kis, L. Törk, K. N. Ross, J. Lamb, W. Read-Button, B. Zheng, H. T. Wang, C. Salt-house, S. J. Haggarty, R. Mazitschek, *Nat. Chem. Biol.* **2016**, *12*, 317 – 323.

[5] a) H. Asanuma, T. Ito, T. Yoshida, X. G. Liang, M. Komiyama, *Angew. Chem. Int. Ed.* **1999**, *38*, 2393 – 2395; *Angew. Chem.* **1999**, *111*, 2547 – 2549; b) H. Asanuma, T. Takarada, T. Yoshida, D. Tamaru, X. G. Liang, M. Komiyama, *Angew. Chem. Int. Ed.* **2001**, *40*, 2671 – 2673; *Angew. Chem.* **2001**, *113*, 2743 – 2745; c) X. G. Liang, H. Asanuma, M. Komiyama, *J. Am. Chem. Soc.* **2002**, *124*, 1877 – 1883; d) H. Asanuma, X. Liang, H. Nishioka, D. Matsunaga, M. Liu, M. Komiyama, *Nat. Protoc.* **2007**, *2*, 203 – 212.

[6] M. Z. Liu, H. Asanuma, M. Komiyama, *J. Am. Chem. Soc.* **2006**, *128*, 1009 – 1015.

[7] D. Matsunaga, H. Asanuma, M. Komiyama, *J. Am. Chem. Soc.* **2004**, *126*, 11452 – 11453.

[8] A. Yamazawa, X. G. Liang, H. Asanuma, M. Komiyama, *Angew. Chem. Int. Ed.* **2000**, *39*, 2356 – 2357; *Angew. Chem.* **2000**, *112*, 2446 – 2447.

[9] T. Tian, Y. Y. Song, J. Q. Wang, B. S. Fu, Z. Y. He, X. Q. Xu, A. L. Li, X. Zhou, S. R. Wang, X. Zhou, *J. Am. Chem. Soc.* **2016**, *138*, 955 – 961.

[10] S. Keiper, J. S. Vyle, *Angew. Chem. Int. Ed.* **2006**, *45*, 3306 – 3309; *Angew. Chem.* **2006**, *118*, 3384 – 3387.

[11] P. Li, G. H. Xie, X.-Y. Kong, Z. Zhang, K. Xiao, L. P. Wen, L. Jiang, *Angew. Chem. Int. Ed.* **2016**, *55*, 15637 – 15641; *Angew. Chem.* **2016**, *128*, 15866 – 15870.

[12] a) Y. Q. Yan, X. Wang, J. I. L. Chen, D. S. Ginger, *J. Am. Chem. Soc.* **2013**, *135*, 8382 – 8387; b) T. Goldau, K. Murayama, C. Brieke, S. Steinwand, P. Mondal, M. Biswas, I. Burghardt, J. Wachtveitl, H. Asanuma, A. Heckel, *Chem. Eur. J.* **2015**, *21*, 2845 – 2854; c) T. Goldau, K. Murayama, C. Brieke, H. Asanuma, A. Heckel, *Chem. Eur. J.* **2015**, *21*, 17870 – 17876; d) A. Kingsland, S. Samai, Y. Yan, D. S. Ginger, L. Maibaum, *J. Phys. Chem. Lett.* **2016**, *7*, 3027 – 3031; e) S. Samai, D. J. Bradley, T. L. Y. Choi, Y. Q. Yan, D. S. Ginger, *J. Phys. Chem. C* **2017**, *121*, 6997 – 7004.

[13] a) M. Biswas, I. Burghardt, *Biophys. J.* **2014**, *107*, 932 – 940; b) D. Rastädter, M. Biswas, I. Burghardt, *J. Phys. Chem. B* **2014**, *118*, 8478 – 8488; c) P. Mondal, M. Biswas, T. Goldau, A. Heckel, I. Burghardt, *J. Phys. Chem. B* **2015**, *119*, 11275 – 11286; d) I. K. Lednev, T. Q. Ye, P. Matousek, M. Towrie, P. Foggi, F. V. R. Neuwahl, S. Umapathy, R. E. Hester, J. N. Moore, *Chem. Phys. Lett.* **1998**, *290*, 68 – 74.

[14] P. Mondal, G. Granucci, D. Rastädter, M. Persico, I. Burghardt, *ChemRxiv* **2018**, https://doi.org/10.26434/chemrxiv.5758665.v1 (deposited Jan 5, 2018).

[15] a) A. Cembran, F. Bernardi, M. Garavelli, L. Gagliardi, G. Orlandi, *J. Am. Chem. Soc.* **2004**, *126*, 3234 – 3243; b) S.-H. Xia, G. L. Cui, W.-H. Fang, W. Thiel, *Angew. Chem. Int. Ed.* **2016**, *55*, 2067 – 2072; *Angew. Chem.* **2016**, *128*, 2107 – 2112; c) T. Cusati, G. Granucci, M. Persico, *J. Am. Chem. Soc.* **2011**, *133*, 5109 – 5123; d) O. Weingart, Z. Lan, A. Koslowski, W. Thiel, *J. Phys. Chem. Lett.* **2011**, *2*, 1506 – 1509; e) M. Pederzoli, J. Pittner, M. Barbatti, H. Lischka, *J. Phys. Chem. A* **2011**, *115*, 11136 – 11143; f) M. Böckmann, N. L. Doltsinis, D. Marx, *Angew. Chem. Int. Ed.* **2010**, *49*, 3382 – 3384; *Angew. Chem.* **2010**, *122*, 3454 – 3456; g) J. A. Gámez, O. Weingart, A. Koslowski, W. Thiel, *J. Chem. Theory Comput.* **2012**, *8*, 2352 – 2358; h) M. Böckmann, N. L. Doltsinis, D. Marx, *J. Phys. Chem. A* **2010**, *114*, 745 – 754; i) T. Schultz, J. Quenneville, B. Levine, A. Toniolo, T. J. Martínez, S. Lochbrunner, M. Schmitt, J. P. Shaffer, M. Z. Zgierski, A. Stolow, *J. Am. Chem. Soc.* **2003**, *125*, 8098 – 8099; j) A. Toniolo, C. Ciminelli, M. Persico, T. J. Martínez, *J. Chem. Phys.* **2005**, *123*, 234308; k) T. Fujino, S. Arzhantsev, T. Tahara, *J. Phys. Chem. A* **2001**, *105*, 8123 – 8129.